Insights from techno-economic analysis can guide the design of low-temperature CO_2 electrolyzers towards industrial scaleup

Shashwati C. da Cunha[1], Joaquin Resasco[1]*

1. McKetta Department of Chemical Engineering, The University of Texas at Austin, Austin, TX 78712, USA

*Corresponding author: resasco@utexas.edu

Abstract

The field of CO_2 reduction has identified several challenges that must be overcome to realize its immense potential to simultaneously close the carbon cycle, replace fossil-based chemical feedstocks, and store renewable electricity. However, frequently cited research targets were set without quantitatively predicting their impact on the economic viability of CO_2 reduction. Using a physics-informed techno-economic assessment, we offer guidance on the most pressing research priorities for CO_2 reduction based on state-of-the-art electrolyzer performance. We find that the levelized product cost is dominated by the cost of electricity used to drive electrolysis, and the capital cost of the process mostly arises from separations, especially of unreacted CO_2 to be recycled. At a cell resistance as low as 1 $\Omega \cdot cm^2$ and retail electricity prices, operating at a total current density >475 mA/cm^2 drives up electricity demands and increases the cost of producing CO. High current density operation is therefore undesirable unless low cell voltages can be maintained. Although wholesale wind and solar electricity are cheaper than retail electricity, their capacity factors are too low for economical process operation. Adding energy storage to increase the capacity factor of solar electricity triples the capital cost from $34.4 million to $112.6 million for a plant making 50 t_{CO}/day. Improving single-pass conversion is not a priority because it leads to selectivity loss in contemporary membrane electrode assemblies, giving an optimum conversion

at <15%. To overcome this limitation, we identify the opportunity to modify reactor design to improve CO_2 availability to the catalyst. Decoupling selectivity and single-pass conversion by moving away from a plug flow reactor design, without adding cell voltage, would reduce the base case levelized cost of \$1.22/kg_{CO} to \$0.97/kg_{CO} and save 36% on capital cost. Finally, we conclude that resolving the "carbonate crossover problem" in neutral electrolytes is not a priority for improving the levelized cost of product.

Introduction

Low-temperature electrochemical CO_2 reduction (CO_2R) can convert captured carbon dioxide into chemical feedstocks and fuels using renewable electricity and water in an electrolyzer.[1] Academic research focusing on catalyst improvement, membrane testing, and electrolyte design has exploded in the last decade.[2] However, scaleup efforts have been slow because of multiple technical challenges that make the technology too expensive for practical application today. These include limited catalyst activity and selectivity, mechanically unstable or poorly conducting membranes, and undesirable electrolyte crossover and flooding.[3] To advance in technology readiness level, CO_2R experiments focused on overcoming these challenges need to be coupled with process-scale simulations that can identify critical bottlenecks towards economic viability.

As pointed out recently, there is an opportunity for techno-economic and life-cycle analyses to direct technology development in chemical engineering research.[4] For CO_2R, the disconnect between studies at the process and reactor scale is evident in the way that data is collected and reported in the field. Most experimental studies on CO_2 electrolyzers report selectivity almost exclusively on a current basis, without quantifying the flow rates of products relevant for process design. Conversely, many techno-economic assessments (TEAs) for CO_2R processes fail to include models of the electrochemical reactor and therefore neglect key phenomena involved in device operation. As a result, many targets set for the field are not based on technical models, but instead draw on the progression of related technologies like water electrolysis.[1,2,5] Despite important technical differences between water electrolysis and CO_2R, it is often taken for granted that improvements in experimental parameters such as total current density or single-pass conversion will analogously improve overall process economics. However, we have

shown previously that this is not always the case because of interdependencies between key performance indicators unique to CO_2R.[6]

Although many TEAs have been performed on low-temperature CO_2R[7–17], their focus is often on assessing whether the technology is viable in current or future markets. Most TEAs agree that CO_2R is not economical today, but their conclusions from best-case scenarios vary considerably. Since the goal of these studies is often to assess the entire process, analyses generally assume that operating parameters for the electrolyzer, such as cell voltage and current density, are independent. These operating parameters are typically chosen to represent future progress, without considering that dependent variables may consequently change because of governing reactor equations. Furthermore, some TEAs exclude key process units, and most use a 2- to 3-point sensitivity analysis that assumes monotonic trends or even a linear dependence of cost on reactor performance. Some economic assessments have identified technical opportunities, including that low-voltage counterreactions can save costs, especially with inexpensive feedstocks,[18] that alkaline electrolysis is cheaper than acidic if electricity is expensive despite electrolyte regeneration cost,[19] that multiple fluidic compartments and membranes make the payback period impossibly long,[20] and that syngas production is cheaper by making CO and H_2 in two separate electrolyzers than through low-selectivity CO_2R.[21] A few general pathways have also been suggested to achieve economic feasibility.[14,22,23] However, targets for experimental metrics like current density and single-pass conversion have rarely been updated in response to these recommendations.[24]

To guide academic research towards addressing the most challenging problems facing CO_2R scaleup, we conduct a process-scale TEA here based on an analytical reactor model. We examine the sensitivity of process cost to various electrolyzer design parameters, with the aim of

identifying technical improvements that can overcome major limitations in current technology. We confirm that improvements at the materials scale, such as improved membrane conductivity and reduced catalytic overpotentials, are critical. But our analysis also draws attention to the underappreciated need for chemical reactor design to realize commercially viable CO_2R by overcoming reactant transport limitations.

Results

Techno-economic assessment builds on first-principles electrolyzer and process design

In this work, we use a process scale model of CO_2R that incorporates electrolyzer physics to understand how the economics of CO_2R respond to quantitative improvements in materials, reactor, and process design. All results are for low-temperature CO_2R towards CO or ethylene with a neutral, aqueous electrolyte in an anion exchange membrane electrode assembly (MEA) (Figure 1a). For each datapoint, we execute a model of the entire process with a specified rate of production, total current density (j_{total}), and single-pass conversion X_{CO2}. In practice, production rates are fixed to meet contractual obligations, and current density and single-pass conversion are experimentally controlled through the applied potential and feed flow rate. Table 1 shows key specifications for our base case. Next, we estimate the electrolyzer cell voltage from a calculated polarization curve (Figure 1b), and electrolyzer stream compositions based on selectivity and X_{CO2} (Figure 1c). We then use steady-state mass balances to determine the compositions and sizes of all streams according to Figure 1d. CO_2 electrolysis is often operated at unsteady state in neutral electrolytes as salts precipitate in the cathode over time. However, we assume there is a mechanism to frequently redissolve and recover accumulated deposits, such as pulsing water through the

cathode.[25,26] We base capital costs primarily on unit sizes, with the electrolyzer and balance-of-plant modeled from estimations of CO_2R stack manufacturing[27] and the H2A model for water electrolysis.[28] Separation capital cost is scaled relative to a reference unit size.[14] Operating costs are based on standard models for estimating plant costs, including energy, feedstocks, and other working expenses.

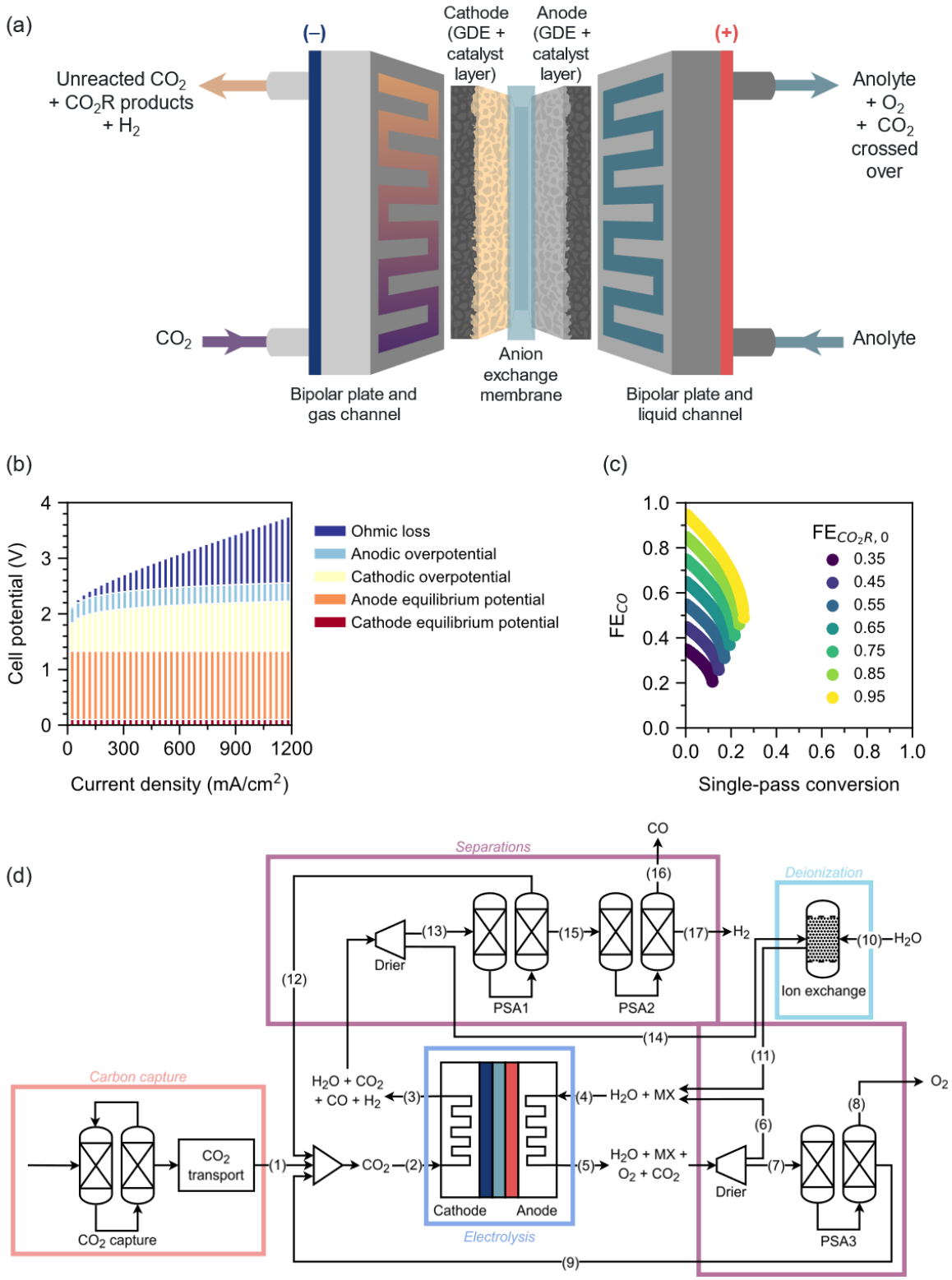

Figure 1. Reactor and process model for low-temperature CO_2R to CO. (a) A three-dimensional representation of the electrolyzer, indicating the stack along the horizontal axis, and the serpentine gas channel delivering CO_2 in the orthogonal plane. The electrolyzer is a membrane electrode assembly in which two gas diffusion electrodes (GDEs) sandwich an anion exchange membrane. (b) Reactor kinetics were modeled electrochemically by generating a

polarization curve, here for CO_2R to CO over Ag coupled with oxygen evolution over IrO_x, separated by an anion exchange membrane. (c) Tradeoff between selectivity (Faradaic efficiency) and single-pass conversion assuming ideal plug flow[29] in the CO_2 channel for an MEA configuration. The model assumes a certain selectivity $FE_{CO2R,\,0}$ in the limit of single-pass conversion $\rightarrow 0$. (d) Process design used for costing. The extraction and purification of CO_2 and water are costed using feedstock costs for captured CO_2 and deionized water, so the corresponding units are excluded from the capital cost. Driers, pressure change units, and tanks are included only as balance-of-plant capital cost, excluding them from operating expenses.

Table 1. Assumptions for the baseline performance of the electrolyzer and process for CO_2R to CO. Sources are detailed throughout the text and in Supplementary Table S3.

Parameter	Symbol	Value	Remarks
Production rate	$\dot{N}_{CO}$	50 metric ton (t_{CO})/day	
Total current density	j_{total}	472 mA/cm^2	Chosen to minimize levelized cost Gives base case cell voltage = 2.92 V (from Eq. 11)
Maximum Faradaic efficiency (at $X_{CO2} \rightarrow 0$)	$FE_{CO2R,\,0}$	95%	
Tafel slope (cathode)	TS_{CO2R}	-230 mV/dec	For Ag
Specific ohmic resistance	ρ	1 Ω·cm^2	Representative anion exchange membrane (50 μm, 0.5 S·cm^2)
Equilibrium cell voltage	E_{cell}	1.34 V	Minimum possible cell voltage (zero resistance, perfect catalysts)
Single-pass conversion of CO_2	X_{CO2}	11.5%	Chosen to minimize levelized cost Together with $FE_{CO2R,\,0}$, gives FE_{CO} = 82% (from Eq. 1)
Carbonate crossover	c	0.5 mol CO_2/ mol e^-	Assumes all ion transport is via CO_3^{2-} anions, and that all generated OH^- equilibrates to CO_3^{2-}
Electricity cost		7.62 ¢/kWh	U.S. average industrial retail electricity price, 2022
Capacity factor	CF	96%	Fraction of operating time per year
Plant lifetime		20 years	Amortization period for capex in levelized cost
Stack lifetime		5 years	Entire electrolyzer capex must be paid again after this period
CO_2 cost		\$75/t_{CO2}	Midrange cost for carbon capture from point sources
Second-law separation efficiency	ζ	7%	Pressure-swing adsorption efficiency
Separation temperature	T_{sep}	313 K	Pressure-swing adsorption temperature

The reactor architecture used for CO_2 electrolysis is typically a stack design originally developed for fuel cells (Figure 1a). Since membrane electrode assembly configurations are usually employed when targeting scaleup, our electrolyzer and process models are based on zero-gap MEA designs. In this configuration, electrodes typically consist of planar nanostructured catalysts supported on gas diffusion layers. The electrodes directly sandwich an ion exchange membrane, resulting in lower resistive losses than in cells with a liquid catholyte. It is common for CO_2R TEAs to specify a full-stack cell voltage, rather than deriving it from first principles. Here, we instead calculate the voltage from a simplified Butler-Volmer model for a membrane electrode assembly, which includes thermodynamic reduction potentials, cathodic and anodic overpotentials (excluding concentration gradients), and membrane resistance (Figure 1b). We focus on CO_2R over silver catalysts to form carbon monoxide, and include results for CO_2R to ethylene over copper in Supplementary Figures S1 – S3.

In most MEAs, CO_2 passes through a serpentine flow channel over the catalyst surface and diffuses through-plane into the gas diffusion layer, in principle evenly utilizing the catalyst. But the timescale of CO_2 diffusion to the catalyst, relative to its convection in the flow channel, leads to a significant CO_2 concentration gradient between the cathode inlet and outlet (Figure 1a).[30,31] This resembles the behavior of a tubular reactor.[29] Increasing the single-pass conversion of CO_2 (X_{CO2}) intensifies this concentration gradient along the length of the reactor. As we have discussed before, this depletion of the available reactant causes a drop in CO_2R selectivity at the expense of the competing hydrogen evolution reaction (HER).[6] Thus, there is a tradeoff between operating at high conversion or high selectivity, a limitation which arises directly from present-day electrolyzer designs. We build this physical tradeoff into our model by relating Faradaic efficiency (FE) to X_{CO2} assuming that the electrolyzer behaves as a plug flow reactor (PFR), following the work of

Hawks et al (Figure 1c).[29] The selectivity is scaled relative to a reference value ($FE_{CO2R,\,0}$), which is the maximum achievable selectivity towards CO_2R in the limit of zero conversion. We assume that hydrogen is the only side product formed.

Depending on the CO_2 electrolyzer configuration, electrolyte, and membrane, the reactor outlet streams vary in number, composition, and size. Consequently, a variety of up- and downstream units are required (Figure 1d). In our calculations, we represent driers, compressors, pumps, and tanks as a balance-of-plant capital cost.[28] Their utilities have been shown to be a small fraction of separation and electrolysis duties,[20] so we also neglect their operating costs here. The cathode outlet is a wet gas consisting of CO_2R products, unreacted CO_2, and H_2 from the HER. When an anion exchange membrane is used, gas separations are required on both sides of the reactor to recycle CO_2 to the inlet. For smaller scale processes, these gas separation units are typically considered to be pressure swing adsorbers (PSA), each of which is selective to one gas. Not all gas mixtures are amenable to selective adsorption, but variations of PSA have been used to separate air and extract CO, H_2 and CO_2 at large scales since at least the 1980s.[32–34] At high throughputs, CO_2 absorption using amine stripping, and distillation for mixed products will likely be cheaper. We explicitly calculate the capital cost of PSA units using a reference capacity and scaling factor.[14] We also model the separation energy consumed in each unit using a second-law separation efficiency.[35] Further details regarding the development of the reactor and process model can be found in the Methods section and Supplementary Notes 1 and 2.

We emphasize that the trends below reflect electrolyzer performance, but the precise numerical values we provide are not meant to be interpreted as guidelines or targets. All our sensitivity analyses are based on changing a single variable independently, whereas variables often change simultaneously in experiments. Our goal is to clarify how physical relationships in the

electrolyzer affect costs, showing a path forward for the field. These conclusions are described in further detail in the following sections.

Capital cost for low-temperature CO_2R to CO is not limiting

Figure 2a describes the sensitivity of capital expenses (capex) to varying individual electrolyzer and process variables for CO_2R to CO. As a baseline, we model a plant producing 50 t_{CO}/day (14.2 MW). This yields a capital cost of $34.4 million. This is not unreasonable for a plant of the given size; a conventional steam methane reforming process for 500 t_{H2}/day requires $547 million to build.[34] Nor is this unreasonably high for the industry – large chemical companies spend $1-4 billion per year on capital.[36] As expected, capex is highly sensitive to production rate, which determines all unit sizes. Since the total production basis is fixed, a lower CO_2R current density requires a larger electrolyzer area. Figure 2b shows a representative breakdown of capex with varying total current density. Reactor capex falls as $(j_{total})^{-1}$ to become much smaller than the capex of separations beyond a certain value, ~500 mA/cm^2 in our model. Consequently, further increases in current density do not significantly reduce capex.

Capex also depends on selectivity, which is controlled by X_{CO2} and $FE_{CO2R,\,0}$. Capex is highly sensitive to changing selectivity, which influences the size of both the electrolyzer and separation units. Given that the production basis is fixed, the total current must be higher if the selectivity is lower, which increases the size of the electrolyzer. Apart from the variables discussed above, capex is largely unaffected by changes within our process design. However, it is sensitive to the cost of electrolyzer per unit area, as shown in Supplementary Figure S4.

Operating cost for CO_2R to CO is controlled by electricity demand and capacity factor

The levelized production cost, which is the combined capex and opex per unit product, is dominated by opex because the capex is amortized over the lifetime of the plant. Over a 20-year horizon, the opex ($19.5 million/year) is 11 times larger than the capex. Further discussions will hence center around the opex, which is far from economical at the current state of the art for CO_2R to CO and ethylene. This cost includes reactants, electric utilities, representative labor and maintenance costs, and overheads. Overheads depend on the plant size and therefore on capital cost. We model the sensitivity of opex to individual electrolyzer and process variables for CO_2R to CO in Figure 2c. The operating j_{total} and X_{CO2} are fixed in Figure 2c, but we also include the sensitivity of costs when optimizing j_{total} and X_{CO2} in Supplementary Figure S5. The conclusions from this paper are valid even when the operating points are optimized.

We find that the dominant operating expense is electricity (Figure 2d), in line with previous studies.[9,11] Retail industrial electricity prices in the United States average 7 – 9 ¢/kWh,[37] but CO_2R to CO requires nearly free electricity to break even in our model (Figure 2d). We do not include any cost of onsite utilities – electricity costs are assumed to be as purchased (retail pricing), affecting opex only. In contrast to our model, many TEAs on CO_2R use wholesale renewable electricity prices (<3 ¢/kWh) but assume a high capacity factor (>90%). These electricity prices are based on solar and wind farms that have capacity factors in the 20 – 30% range because of hourly and seasonal variations.[38,39] Figure 2e shows that even using cheap wholesale solar electricity, high capacity factors are required to make CO_2R economical. Therefore, the scenario modeled in these studies is only feasible with massive energy storage capacity in the system to buffer times when renewables are unavailable, in addition to onsite generation. The capital costs associated with this scale of energy storage far outweigh the capex of the CO_2R process itself

(Figure 3a). Despite this capex associated with increasing the capacity factor, it is more economical than operating the electrolyzer at low capacity factors, whether the energy storage is modeled inside (Figure 3b) or outside (Figure 3c) the process limits. The source of electricity also controls the carbon intensity of the process. Normalized over the lifetime of the plant, the resulting cost of CO_2 capture and utilization is \$776/t_{CO2} at the base case retail electricity price, and after product sales is \$375/t_{CO2}. A fraction of the electricity mix must be fossil-free for carbon-neutral operation of CO_2R, since the grid carbon intensity must be <0.16 kg_{CO2}/kWh at the base case (Supplementary Figure S6).

To evaluate strategies to reduce electricity demand, we break down the total energy consumption of the system in Figure 2f. Process energy is dominated by the electrolyzer under all relevant conditions shown here. The polarization curve for CO_2R (Figure 1b) gives a much higher cell voltage than the most analogous industrial process, water electrolysis to produce green hydrogen. The minimum cell voltage, 1.34 V, arises thermodynamically and is mostly contributed by the standard oxidation potential of water. For all other parameters at the base case, a hypothetical cell running at 1.34 V yields an operating cost of \$0.83/kg_{CO} (Figure 2c), still higher than the product price. This minimum voltage could be reduced by considering alternative oxidation reactions, especially ones with inexpensive feedstocks[40]. Improvements can also be made to the equilibrium reaction conditions by modulating temperature, pH, and surface concentration, which is beyond the scope of this work.

Another major energy demand comes from sluggish cathode reaction kinetics, represented by the high cathodic overpotential, even without introducing concentration overpotential from limited CO_2 solubility. The cathode overpotential contributes to a high voltage demand, even at low current densities. The third major contributor is membrane resistance. Anion exchange

membranes (area-specific resistance ~0.2 – 1 $\Omega \cdot cm^2$)[41–43] do not exhibit the same stability and conductivity as proton exchange membranes (typically Nafion™ derivatives, area-specific resistance ~0.1 – 0.3 $\Omega \cdot cm^2$)[44]. Consequently, thicker membranes are required with higher through-plane resistances than those used in water electrolysis, leading to higher resistive losses.

Since 78% of process energy goes towards electrolysis (Figure 2f), opex is barely affected by eliminating CO_2 crossover to save on anode gas separation. If there is any voltage or selectivity loss associated with eliminating carbonate crossover, the beneficial effect on separation cost is overwhelmed by additional energy demands from the electrolyzer. Even capex, which is dominated by separation cost, mostly depends on single-pass conversion. Since the O_2/CO_2 stream from the anode is the smallest PSA inlet, eliminating crossover does not notably influence the capex.

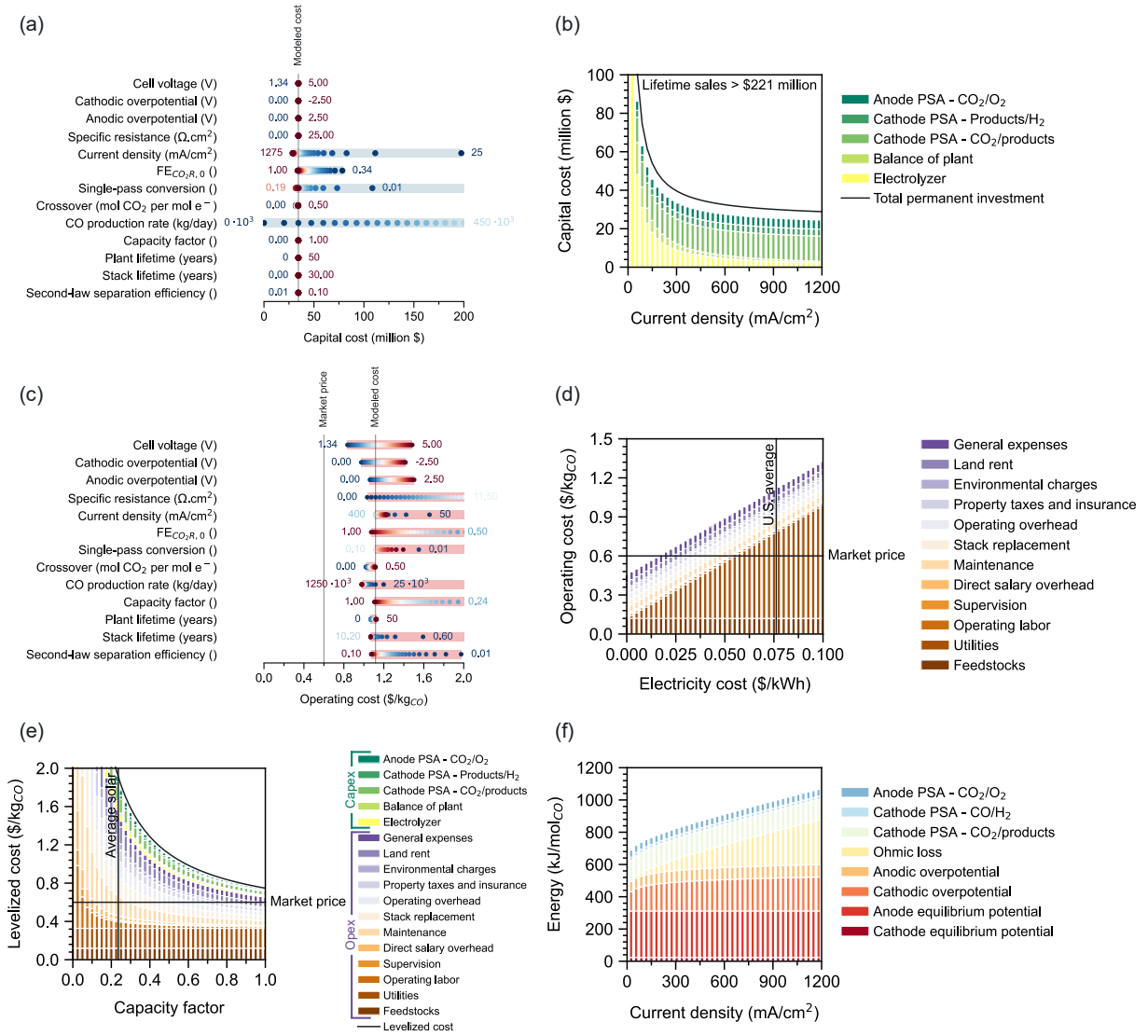

242

243 **Figure 2. Cost breakdown for CO_2R to CO for a 50 t_{CO}/day process.** (a) Single-variable sensitivity of capital cost
244 shows that the base case capital cost is reasonable for the plant size. Vertical lines mark the market price for CO and
245 the modeled cost at the base case scenario. Each horizontal bar indicates the range in cost upon changing one given
246 variable in the model, holding all others at the base case. Variable values at the best and worst costs are labeled at the
247 ends of the bar. For instance, a total current density of 1275 mA/cm^2 gives the lowest capital cost, 25 mA/cm^2 the
248 highest, and the base case is 472 mA/cm^2. (b) Cost breakdown for sensitivity of capital cost to current density. Capex
249 mostly arises from gas separations, so increasing current density to reduce electrolyzer area is only relevant upto
250 moderate current densities. (c) Single-variable sensitivity analysis for operating cost of CO_2R to CO. Opex changes
251 non-monotonically against total current density and single-pass conversion, exhibiting an optimum in both. (d) The
252 overall cost of CO_2R is not yet comparable to the market price[45] for pure CO derived from fossil sources. Electricity
253 would need to be much cheaper than US average industrial retail electricity today, almost free, to break even in a
254 current state-of-the-art electrolyzer. (e) Even if cheap wholesale solar electricity at $0.024/kWh is available, the
255 required plant capacity factor to break even far exceeds the solar capacity factor. (f) A breakdown of energy
256 (electricity) demands for the process shows that electrolysis dominates over separations. Energy requirements come
257 from sluggish CO_2R kinetics, thermodynamics of the unfavorable oxygen evolution, and membrane resistance.

All analyses use a base electricity price of \$0.076/kWh, carbon dioxide feedstock at \$75/t_{CO2}, 20-year plant lifetime, and single-pass conversion of 11.5%. Supplementary Table S3 lists other assumptions for the baseline and Supplementary Table S4 gives the evaluated points for each variable in the sensitivity analyses.

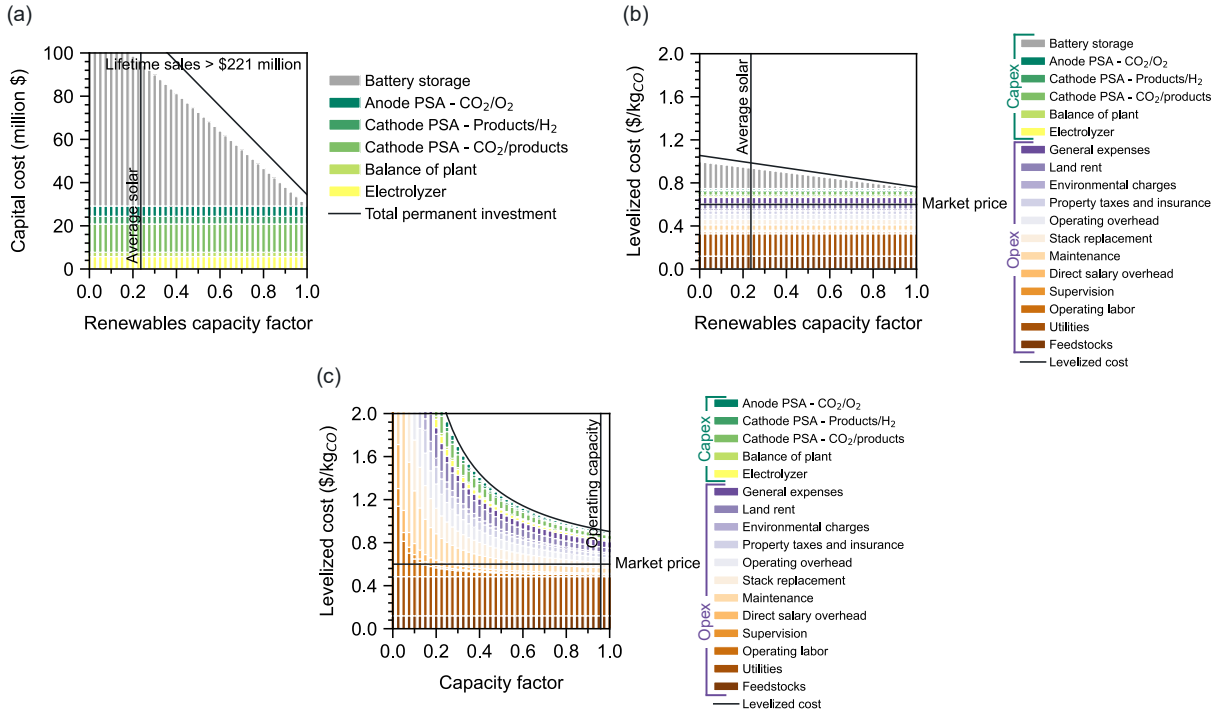

Figure 3. Cost of energy storage coupled to renewable electricity for CO_2R to CO. (a) Capital cost breakdown for a plant powered by intermittently available electricity, with an additional capital cost for energy storage. The additional capex for a battery system is \$200/kWh, which is based on future projections from the National Renewable Energy Laboratory.[46] (b) The levelized cost of CO_2R powered by solar photovoltaics is much lower with the inclusion of battery storage, despite its enormous capital cost. This shows the importance of operating such a plant at high capacity. Solar electricity costs \$0.024/kWh[47], about a third of current retail electricity prices. (c) A similar levelized cost is obtained for a plant operating at 96% capacity by using the utility cost of wind energy with storage (\$0.042/kWh)[47], i.e. no additional capex, but adjusting the opex to purchase from a wind farm with utility-scale storage.

All analyses use a single-pass conversion of 11.5%, current density of 472 mA/cm^2, carbon dioxide feedstock at \$75/t_{CO2}, and a 20-year plant lifetime. The intended capacity factor of the plant is 96%.

Increasing current density without lowering cell voltage increases cost

Next, we examine the non-monotonic trend in cost with current density, which reveals an optimal operating point (Figure 4). The field has targeted increasingly high current density operation, often >1.5 A/cm^2 of total or partial current density. These current densities require high cell voltages and challenge cell stability as it becomes difficult to maintain uniform reaction rates, temperatures through the electrolyzer, and electrode wetting. But our analysis shows that operating at high current densities will not bring CO_2R costs down. Rather than operating at a higher point on the polarization curve, the curve itself must be lowered. Given a fixed production basis, increasing the current density does reduce the capex and capex-dependent opex, since a smaller electrolyzer area is required. But this benefit is eventually outweighed by the increased ohmic resistance in the electrolyzer, which grows linearly with current density. Therefore, a tradeoff arises between utility cost and capex-dependent opex (Figure 4a). The resulting minimum occurs at just 300 – 600 mA/cm^2 for current electricity prices, 472 mA/cm^2 for our base case. Both sides of this tradeoff are non-linear, since electrolyzer capex is area-dependent and the polarization curve is nonlinear, especially at low current densities. Supplementary Figure S7 shows that the optimum is sensitive to electrolyzer cost; if the electrolyzer is more expensive, higher current densities are favorable. It also shows the relatively small variation in the optimum current density with production rate, driven again by capex increases.

The optimal operating current density depends on the cost of electricity (Figure 4b). Even with cheap electricity (3 ¢/kWh), the optimal current density is 750 mA/cm^2 if all other variables are held at their base case values. The tradeoff also depends on the cell resistance (Figure 4c), which determines the slope of the polarization curve at high voltages. Increasing the specific resistance from 1 to 2 Ω·cm^2 shifts the optimal current density to <350 mA/cm^2. Furthermore, our

model does not account for the overpotential required for hydrogen evolution, making the cell voltages an underestimate, especially at high current density.[48] Without reducing cell resistance or kinetic overpotentials, high current density operation will make process costs worse, unless accompanied by much lower electricity costs. The literature rarely addresses this tradeoff because many TEAs assume monotonic trends between cost and current density, and use low electricity costs. The downside of high current density operation can only be identified in models that include physical tradeoffs and realistic electricity prices,[49] emphasizing the need to capture physical phenomena within the electrolyzer in TEAs.

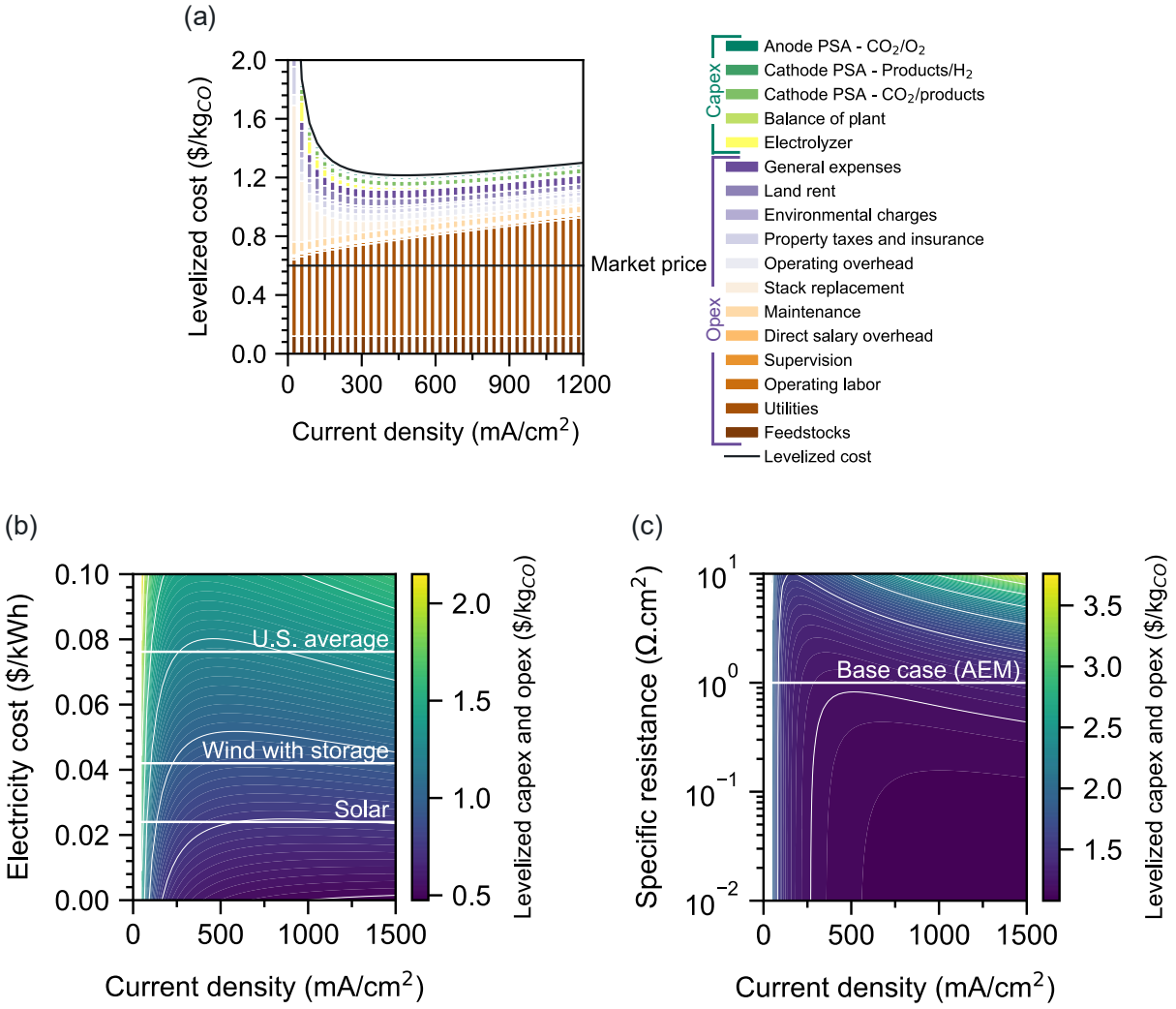

Figure 4. Optimal current density for operating CO_2R to CO. (a) The optimal current density for CO_2 reduction arises from a tradeoff between capex-dependent opex and energy cost. Overheads and levelized capex are large at low current densities since the electrolyzer size necessary to produce a fixed basis, here 50 t_{CO}/day, is bigger. As current density increases, the cell requires higher voltages, increasing utility costs. (b) Electricity cost scales the energy requirement, so the optimal current density is sensitive to it. This heatmap shows that cheaper electricity encourages higher current density operation. However, even at 3 ¢/kWh, operating above 750 mA/cm^2 increases the levelized cost unless the polarization curve is lowered. (c) Cell resistance determines the slope of the polarization curve at high current densities. Reducing membrane resistance would allow higher current density operation, but an increase from 1 to 2 Ω·cm^2 leads to an optimal current density <350 mA/cm^2. In contrast, water electrolyzers operate in the 0.1 Ω·cm^2 range, where ohmic penalties are low and large operating currents are desirable.

Figures (b) and (c) are based on uniform 51×51 grids in the x- and y-axes. All analyses use a single-pass conversion of 11.5%, carbon dioxide feedstock at \$75/t_{CO2}, and 20-year plant lifetime. Figures (a) and (c) use a base electricity price of \$0.076/kWh.

Electrolyzer redesign is an opportunity to maintain selectivity at high single-pass conversion

Our findings support recent work suggesting that reactor design significantly affects electrolyzer performance, especially when scaling up.[30,31] Although selectivities near 100% can already be achieved for CO_2R to CO at ultra-low conversions, increasing X_{CO2} leads to poor availability of CO_2 to the catalyst, causing selectivity loss.[6] Selectivity impacts product cost because low selectivity wastes electrolyzer energy on making hydrogen. Herein, we explicitly define selectivity as a function of the specified X_{CO2} (Figure 1c). To quantitatively describe the relationship between selectivity and X_{CO2}, we use an approach developed by Hawks et al.[29] This model describes the electrolyzer gas channel as a one-dimensional plug flow reactor with first-order CO_2 consumption through reduction and carbonate crossover, and is validated by several MEA experiments.[50–53] We assume that the high pH at the cathode surface causes all generated OH^-, whether from CO_2R or hydrogen evolution, to form CO_3^{2-} by stoichiometrically consuming CO_2.[41] The limiting single-pass conversion (x-limit in Figures 5a, 5d, and 5i) results from the steady-state mass balance on CO_2 imposed by this assumption. Other models have been proposed to capture this behavior as well,[49] but we chose this model to independently account for operating variables, specifically flow rate and total current or cell voltage.

The resulting tradeoff between selectivity and X_{CO2} is steep (Figure 5a), leading to an expensive process with an optimal operating point at low conversion (Figure 5b). This behavior has been observed in prior studies as well.[35] The steepness of the tradeoff arises entirely from the plug flow design of the reactor, which depletes CO_2 along its length and increases HER selectivity. Figure 5c shows that if constrained by this relationship, improvements will be needed across multiple variables to make CO_2R comparable to current market prices. Except Figures 5d – i, other results in this paper are based on this strict plug flow relationship.

Different reactor configurations can overcome plug flow limitations, changing the FE_{CO}-X_{CO2} relationship. Moving from a zero-gap MEA (Figures 5a – c) to a flow cell (Figures 5d – f) of Kas et al[31] levels out the steep tradeoff, as shown in Figure 5d. While the MEA is fed only CO_2 to the cathode, the flow cell also uses a 1 M $KHCO_3$ catholyte feed which contributes to the (bi)carbonate equilibrium. If there is no recirculation, the buffering catholyte maintains CO_2 concentration along the length of the reactor. Consequently, operating near the maximum achievable X_{CO2} becomes preferable with the optimum $X_{CO2} > 20\%$ (Figure 5e). Here, we maintain the crossover at its value of 0.5 mol_{CO2}/mol_{e-}. However, the use of a catholyte in a flow cell configuration introduces considerable challenges, including increased cell voltage, mechanical instability, and additional electrolyte cost.[54] We capture these difficulties coarsely by increasing the cell resistance from 1 $\Omega \cdot cm^2$ to 16.67 $\Omega \cdot cm^2$ between Figures 5a – c to Figures 5d – f.[42] Therefore, the accessible cost in Figure 5f is even higher, requiring major improvements. This levelized cost can only be achieved at a low current density (126 mA/cm^2), driving a large capex of $45 million at the baseline of Figure 5f. The electrolyzer alone costs $19 million since its area is triple that of the MEA from Figure 5c.

However, the field of reactor design for CO_2R is relatively unexplored from the lens of improving selectivity and overall process cost. We emphasize that reactor design is an immense opportunity for the field to improve the performance of CO_2 electrolyzers. This is illustrated in Figures 5g – i for a hypothetical reactor design that maintains the conductivity of an MEA (~1 $\Omega \cdot cm^2$) while changing the CO_2 supply to maintain catalyst performance along the bed. Without any improvement in catalysts, membranes, or market conditions, a less steep FE_{CO}-X_{CO2} curve (Figure 5g) lowers the cost of CO from $1.22/$kg_{CO}$ in the PFR base case (Figure 5b) to $0.97/$kg_{CO}$ (Figure 5h). This change is achieved by moving the optimal X_{CO2} to 41.0% while maintaining

FE_{CO2R} at 91%. Apart from saving \$0.21/kg_{CO} in opex, the capital cost is lowered by 36% to \$22 million. Figure 5i shows that with small further improvements, CO_2R in this reactor design can approach the market price. This design could be achieved using an MEA with alternate CO_2 supply patterns that improve catalyst utilization, such as parallel or point flow configurations,[55–57] or a number of novel configurations that are yet untested. There are also opportunities in changing catalyst selectivity along the bed to optimize electrolyzer cost, or in resizing flow paths or redesigning gas diffusion media to improve catalyst utilization across the electrode area.

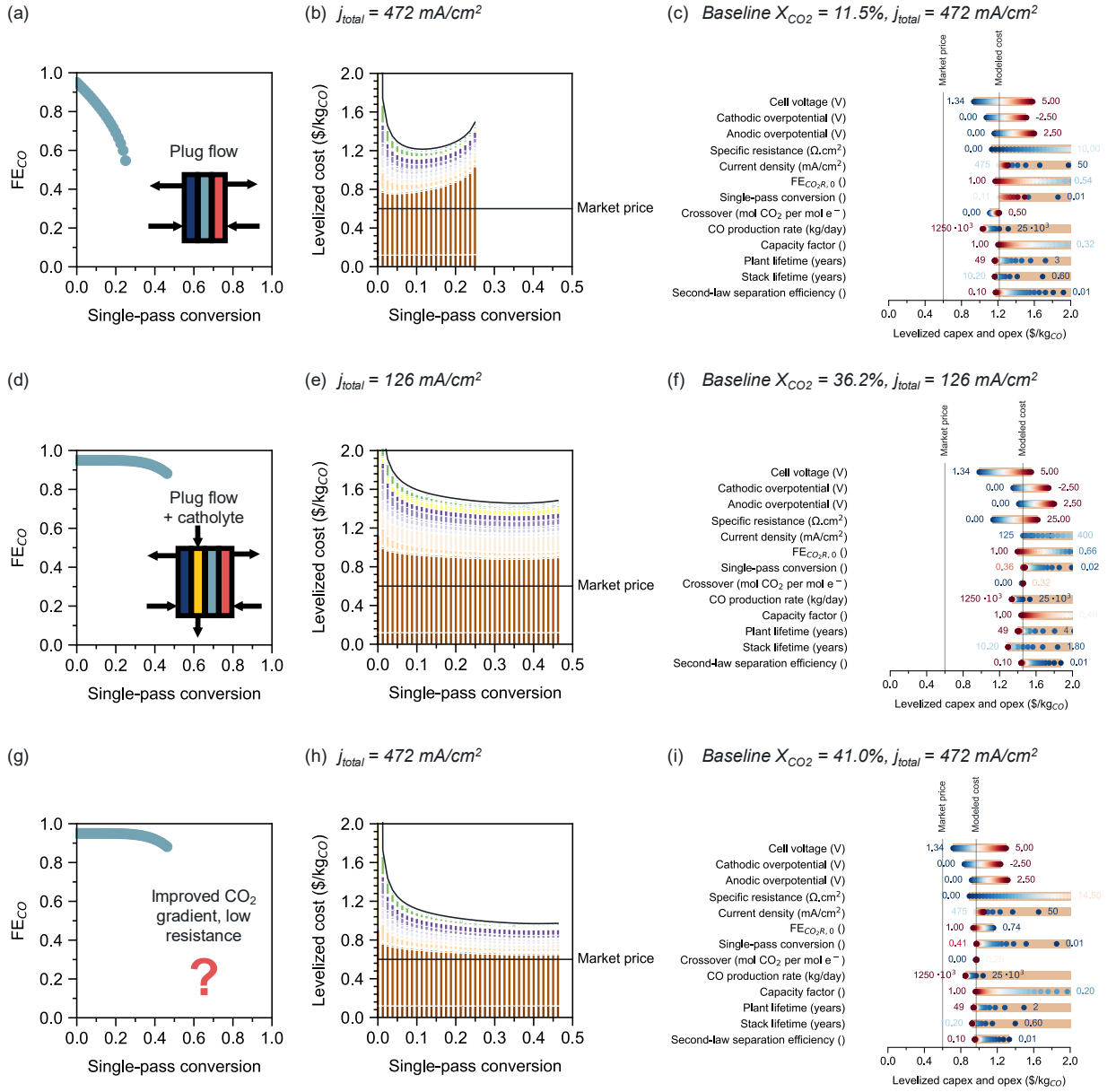

Figure 5. Reactor design is an opportunity for CO_2R to CO to become economical. Figures (a) – (c) are for a membrane electrode assembly configuration; (d) – (f) for a flow cell; and (g) – (i) for a future reactor design. (a) There is a steep loss in selectivity with single-pass conversion if the electrolyzer has plug flow characteristics, as in MEAs with linear flow paths (Hawks et al.[29]) This relationship is used throughout the paper. (b) The steep tradeoff results in expensive products; the optimal single-pass conversion is <15%. (c) Univariate sensitivity of the levelized cost in a current MEA to reactor and process parameters suggests that the process may not be economical even with improvements to multiple parameters. (d) Tradeoff between selectivity and single-pass conversion for a flow reactor configuration with bicarbonate electrolyte contacting the cathode, adapted from continuum modeling by Kas et al.[31] The catholyte levels the curve by adding another source of CO_2 to the catalyst, namely the equilibration of bicarbonate electrolyte into CO_2 when the gas is depleted by reaction. (e) If the FE_{CO}-X_{CO2} curve is more level, a much higher single-pass conversion is optimal. However, the 17× increase in cell resistance for the flow cell versus the MEA case leads to worse economics. (f) It is unlikely that flow cell operation would be economical without major improvements in reactor performance. (g) MEA redesign would be able to maintain selectivity at higher conversion through reaction engineering that improves CO_2 availability across the cathode surface, without increasing cell resistance. (h) Without

any improvement in catalysts or membranes, this redesign closes the gap between the production cost and sale price by 40%. (i) With reactor redesign, the modeled base case cost of CO_2R is much closer to the market price than any other scenario. Since \$0.21/kg_{CO} is saved in opex and \$12 million in capex, smaller improvements are required to make CO_2R economical. Therefore, we point to the impact of changing the relationship between selectivity and single-pass conversion as an important control of process cost.

Legends for (b), (e) and (h) are the same as in Figures 2e and 3a; Figure 2 describes single-variable sensitivity figures. All analyses use a base electricity price of \$0.076/kWh and carbon dioxide feedstock at \$75/t_{CO2}.

Conclusions

In this paper, we conduct a techno-economic assessment of low-temperature CO_2 reduction in an MEA. Our goal is to inform the direction of experimental research, rather than assessing the practicality of the technology itself. By coupling a physical model of an electrolyzer with a process model, we provide insights on the most important levers that the field should aim to control. As previously shown, electrolyzer energy is the largest contributor to the levelized cost of product ($/kg). This energy requirement arises from catalyst kinetics for CO_2R, the resistance of anion exchange membranes, and the thermodynamics of the anodic oxygen evolution reaction. However, we note that operating at a higher current density, even with fixed selectivity, does not result in better economics for a given production rate, unless the required cell voltage is lower. At cell resistances $\geq 1\ \Omega \cdot cm^2$, operating above 475 mA/cm^2 is detrimental to the levelized cost of the process.

Unlike many previous assessments, we use state-of-the-art electrolyzer design as the baseline for our model. This means that CO_2 is supplied to the MEA through a serpentine flow path that leads to concentration gradients along the electrode surface. We find that this relationship is an important and largely unexplored opportunity to improve the economics of CO_2R. Current MEA designs are derived from fuel cells and water electrolyzers, which do not have the same selectivity considerations as CO_2R, nor the same multiphase behavior. There is enormous potential for reaction engineering in these systems that can draw from years of work on process intensification for thermal reactors. The early history of electrochemical CO_2 reduction was marked by seminal advances in understanding reaction chemistry[58,59]; we now propose a great opportunity for chemical reaction engineering to leave a historic mark in the field.

We also use the current cost of grid electricity throughout. This is because low capacity factors, typical for direct use of solar and wind, make economical operation impossible, even if electricity is cheaper. Our cost estimates for electricity are hence much higher than previous estimates. However, our model suffers from some limitations, which have been discussed and addressed elsewhere. Firstly, the plug flow model of Hawks et al.[29] makes some assumptions, notably that volumetric flowrate is fixed along the length of the reactor. While this is unrealistic at high X_{CO2}, removing this assumption would lead to an even steeper tradeoff than we have used. Furthermore, nearly all CO_2 reduction occurs early in the flow path, justifying the assumption. More generally, we have assumed a design for the cell that is only directly applicable to linear flow paths with neutral electrolytes and an anion exchange membrane. Second, we set a total current density which controls cell voltage, and a single-pass conversion which controls selectivity and feed flow rate. Realistically, the feed flow rate and cell voltage are set, and in turn control current density and selectivity. We chose this model to avoid the complex inverse problem of breaking down a full-cell voltage into its components. The relationships for selectivity and single-pass conversion have been shown to hold up to the assumption of independence from the cell voltage.[29,35] Thirdly, we make simplifying assumptions in the process, by ignoring the duties associated with temperature and pressure changes, and any product delivery specifications such as pressure and water content. Further, we do not use any depreciation of fixed equipment when representing the levelized cost, since the process is unprofitable with a net present value of -$72.0 million (Supplementary Figures S8 – 9). We do not correct prices for various years via a price index. We also assume that CO_2R products are purely binary mixes of H_2 with either CO or ethylene. Today, CO_2R to ethylene produces other gases and liquids that are not addressed by this model. However, we show here that single-step CO_2R to ethylene is not economical even without

443 these complications, with a levelized cost of \$7.64/$kg_{ethylene}$ and capital cost of \$180 million
444 (Supplementary Figures S1 – S3).

445 All models have limitations, and we do not intend to use ours to provide a target "number"
446 for current density or conversion for researchers to pursue. Rather, we seek to identify the trends
447 in cost with reactor design, and to provide insights to guide the direction of future research. In this
448 context, we make the following recommendations to the field. Firstly, it is critical that we explore
449 other strategies for bulk transport of reactants and products to the electrode by considering reactor
450 designs that overcome plug flow. Secondly, electricity costs today are prohibitively high. Although
451 renewable electricity can be cheaper, operating at their low capacity factors is also prohibitively
452 expensive. We must therefore consider the possibility of offering multiple services through
453 electrolysis, including carbon utilization credits, offsetting the cannibalization of solar and wind
454 farms that causes negative electricity pricing, and demand response in electric grids. This means
455 we must work on power-responsive operation of electrolyzers that can handle rapid startup,
456 ramping and shutdown, rather than fixed current density operation. Lastly, we have shown that
457 phenomena at the reactor scale dramatically affect the overall economics for CO_2R. Techno-
458 economic assessments would benefit from incorporating more detailed fundamental models of
459 electrolyzer phenomena. Tradeoffs that are fundamental to current electrolyzer design are often
460 erased by using representative "optimistic" and "base case" datapoints based on independent
461 experiments. Instead, incorporating these tradeoffs and non-monotonic trends can identify the most
462 critical needs for the field to make progress.

Methods

Each cost datapoint in this paper (i.e., bar in bar charts, point in sensitivity plot, point on contoured heatmap) is generated from a single run of the following model. The Python model is provided as Supplementary Software. A number of constants and parameters are imported into it via the Supplementary Workbook.

Electrolyzer model

The electrolyzer unit is assumed to be a membrane electrode assembly, since this configuration is amenable to stacking and minimizes cell voltage. Even where flow cells are referenced (Figures 5d – f), the voltametric model is an MEA design, but with a higher resistance introduced to represent both the membrane and electrolyte. We first choose a single-pass conversion, X_{CO2}, and use it to determine the electrolyzer selectivity by numerically solving for FE_{CO2R} in the following equation (Supplementary Figure S10):

$$\frac{FE_{CO_2R}}{FE_{CO_2R,\,0}} + \frac{X_{CO_2}\left(1+\frac{n\cdot c}{FE_{CO_2R}\cdot z}\right)}{\ln\left(1-X_{CO_2}\left(1+\frac{n\cdot c}{FE_{CO_2R}\cdot z}\right)\right)} = 0 \qquad \text{Eq. 1}$$

where FE_{CO2R} is the Faradaic or current efficiency towards the given product, $FE_{CO2R,0}$ is the selectivity towards the product in the limit of single-pass conversion (X_{CO2}) → 0 (95% towards CO in the base case), n electrons are transferred per mole of product (n = 2 for CO_2R to CO), c is the moles of CO_2 crossed over through the membrane per electron transfer in reaction (c = 0.5 mol CO_2/ mol e^- if all generated OH^- is converted into CO_3^{2-}), and z is the number of CO_2 molecules per product molecule (z = 1 mol_{CO2}/mol_{CO}, 2 mol_{CO2}/mol_{C2H4}). This equation is a mass balance for CO_2 on a fraction of feed basis, derived from plug flow operation for a reaction with first-order kinetics, assuming that the total current density is the same at X_{CO2} → 0 and at the given X_{CO2}. [29,35]

A further derivation is provided in Supplementary Note 1, as well as an explanation of conditions where the model yields values of X_{CO2} or FE_{CO2R} which are non-physical. The remaining current is assumed to go towards producing hydrogen, such that:

$$FE_{H2} = 1 - FE_{CO2R} \qquad \text{Eq. 2}$$

As a basis, we choose a production rate in $kg_{product}$/day, which is converted through Faraday's law into a total current:

$$i_{CO2R} = nF\dot{N}_{product\,(16)} \qquad \text{Eq. 3}$$

where i_{CO2R} is the current towards the CO_2R products, F is Faraday's constant (96,498 C/ mol e^-), and $\dot{N}$ is the molar production rate of CO_2R products.

This gives the total current as well as hydrogen and oxygen currents:

$$i_{total} = \frac{i_{CO2R}}{FE_{CO2R}} \qquad \text{Eq. 4}$$

$$i_{H2} = i_{total} - i_{CO2R} \qquad \text{Eq. 5}$$

$$i_{O2} = i_{total} \qquad \text{Eq. 6}$$

We specify an operating current density j_{total}, so the electrolyzer area is now completely specified:

$$A = \frac{i_{total}}{j_{total}} \qquad \text{Eq. 7}$$

where A is the active (electrode) area of the electrolyzer. Although this area is divided across multiple cells in a stack, the electrolyzer cost scales with total active area.

Then, the current density towards each redox reaction is also specified by dividing their respective partial currents by the electrolyzer area. For most cases, we determine the overpotentials

503 at the cathode and anode using a Tafel relationship to achieve the specified partial current density
504 towards CO_2R and OER, respectively. This approach is based on the method and parameters
505 collected by Shin et al (Supplementary Note 1):[14]

506 $$\eta_{CO2R} = \eta_{CO2R,\ ref} + TS_{CO2R} * \log\left(\frac{j_{CO2R}}{j_{CO2R,\ ref}}\right) \qquad \text{Eq. 8}$$

507 where η_{CO2R} is the cathode overpotential, $\eta_{CO2R,\ ref}$ is a reference overpotential, TS_{CO2R} is the
508 Tafel slope, j_{CO2R} is the current density towards CO_2R, and $j_{CO2R,ref}$ is a reference current density.
509 Eq. 8 and its anodic equivalent are the only overpotential equations used. These overpotentials are
510 added to the equilibrium cell voltage E^0_{cell} at standard conditions, uncorrected by the Nernst
511 equation:

512 $$E^0_{cell} = E^0_{CO2R} - E^0_{OER} \qquad \text{Eq. 9}$$

513 The Nernst equation is not used here because determining surface pH as a function of bulk
514 electrolyte pH is nontrivial – the surface pH varies by several units depending on the current
515 density, buffering capacity, and cell design.[31,60] This would require a separate 2D continuum model
516 for each datapoint in the paper, which adds an unrealistic level of computational complexity, while
517 also reducing the generality of our results. Similarly, we do not include the HER current directly
518 in computing the cell voltage, since it cannot easily be decoupled from complex sources such as
519 CO_2 depletion, intrinsic catalyst selectivity, and poor water management. This leads to an
520 underestimation of the cell voltage, especially in operating regions with high HER currents (such
521 as high total current density or low $FE_{CO2R,\ 0}$).

522 Lastly, we add ohmic resistance:

523 $$E_\Omega = -\frac{i_{total} * \rho}{A} \qquad \text{Eq. 10}$$

where E_{Ω} is the ohmic drop, ρ is the area-specific resistance (in $\Omega \cdot cm^2$), and A is the electrolyzer area. This gives the full cell voltage:

$$E_{cell} = E^0_{CO2R} + \eta_{CO2R} - E^0_{OER} - \eta_{OER} + E_{\Omega} \qquad \text{Eq. 11}$$

Then the energy consumed by the electrolyzer per unit product is given by:

$$\text{Energy per mole product} = \frac{E_{cell} * i_{total}}{\dot{N}_{product\ (16)}} \qquad \text{Eq. 12}$$

Process model

Stream compositions in the electrolyzer are determined based on X_{CO2}, selectivity, and crossover as described in Supplementary Note 2. Figure 1d specifies the stream numbers discussed in the following calculations. The fresh CO_2 feed (stream 1) is determined from an overall carbon mass balance, assuming that all carbon eventually exits the system in the form of the product at its fixed production basis (in stream 16). The true inlet feed to the electrolyzer (stream 2) includes recycled CO_2 and is thus determined from the single-pass conversion. Water is fed to the anode (stream 4) in a vast molar excess of 2500× times the OER rate. It is recirculated through streams 6, 11, and 14. Since water is regenerated within the net CO_2 reduction reaction (like $CO_2 \rightarrow CO + ½O_2$), it is only consumed via the hydrogen evolution reaction. At high CO_2R selectivity, the fresh water feed (stream 10) is hence small. Water is recycled via the driers, which are not modeled as units here, but are assumed to have 100% recovery. Molar flow rates of hydrogen, the CO_2R product, and oxygen are determined in electrolyzer outlet streams 3 and 5, and product streams 16, 17 and 8, using their partial currents via Faraday's law (Eq. 3). The crossover ratio c is used to calculate the molar flow rate of CO_2 that crosses through the membrane into stream 5:

$$\dot{N}_{CO_2(5)} = c * \frac{i_{total}}{F} \qquad \text{Eq. 13}$$

where c = 0.5 mol CO_2/ mol e^- for a neutral electrolyte with an anion exchange membrane. This value is based on the stoichiometry of the following homogeneous buffering reaction, occurring at the cathode:

$$CO_2 + 2OH^- \rightarrow CO_3^{2-} + H_2O \qquad \text{Eq. 14}$$

We assume that this reaction consumes all hydroxide generated by the reduction reactions occurring via proton-coupled electron transfers at the surface. Other components around the electrolyzer are determined via elemental and species mass balances. Supplementary Figure S11 shows a process flow diagram annotated with stream flow information at the base case.

Separations via pressure-swing adsorption are modeled to be 100% selective to a single gas; their real selectivity is >95% for relevant cases.[33] The ideal work of separation of a binary gas mixture is adjusted by the second-law efficiency to determine the separation energy:

$$W_{sep}^{ideal} = R * T_{sep} * (x * \ln x + (1 - x) * \ln (1 - x)) \qquad \text{Eq. 15}$$

$$W_{sep}^{real} = \frac{W_{sep}^{ideal}}{\zeta} \qquad \text{Eq. 16}$$

where W_{sep}^{ideal} and W_{sep}^{real} are the ideal and real work of separation per mole of gas mixture respectively, R is the gas constant (8.314 J/mol·K), T_{sep} is the separation temperature (313 K), x is the mole fraction of one of the binary components as determined from a mass balance, and ζ is the second-law separation efficiency (7% at the base case).

Economic model

Supplementary Note 3, with Supplementary Tables S1 and S2, detail our implementation of Sinnott and Towler's framework for process costing.[36] The costs we obtained are similar using

565 the modeling framework of Seider et. al. (Supplementary Figure S12).[61] Capex (capital cost) is
566 calculated for each process unit. Electrolyzer costing is based on manufacturing analysis by
567 Badgett et al.[27], i.e. \$5000/m^2, with balance of plant representing an additional 35% of the cost of
568 the electrolyzer as per the H2A model[28,62]. Pressure-swing adsorbers were priced based on a
569 reference cost of ~\$2 million for a 1000 m^3/hr capacity with a scaling factor of 0.7.[14] Molar stream
570 flow rates were converted into volumetric flows via the ideal gas law assuming a stream pressure
571 of 1 atm and temperature of 313 K. For reference, the volumetric flow rate of the cathode gas outlet
572 at the base case (X_{CO2} = 11.5%, FE_{CO} = 82%) is ~15,510 m^3/hr (595,276 scf). Allocated cost is
573 zero unless there is utility-scale energy storage in the system, as in Figures 3a and 3b. No land
574 purchase cost is included in capex, nor are any other offsite utilities constructed. Rent is included
575 in opex.

576 Opex is composed of costs for feedstocks, utilities, operations, maintenance, overheads,
577 taxes and insurance, and general expenses. These are modeled using standard process design
578 guidelines, not accounting for any differences that may arise from modeling costs for
579 electrochemical processes, like overheads scaling by area or unit number rather than volume.
580 Feedstocks are based on a CO_2 capture cost per ton and the cost of deionized water. The sensitivity
581 of CO_2R cost to these market variables is shown in Supplementary Figure S4. Utilities are
582 calculated from the total energy consumed by the electrolyzer and PSA units, all of which is
583 assumed to be electricity with no heating or cooling duties. Maintenance includes stack
584 replacement, for which the entire electrolyzer capex (with installation) is paid at a regular interval,
585 and 4% of the remaining installed capex. Other overheads are described in Supplementary Note 3.
586 Supplementary Figures S13 – S15 show the sensitivity of capex, opex, and levelized cost to
587 changing electrolyzer, process, and market variables for the three cases shown in Figure 5.

Acknowledgements

The authors acknowledge the support for this work provided by the National Science Foundation under Cooperative Agreement No. EEC-1647722, an Engineering Research Center for the Innovative and Strategic Transformation of Alkane Resources (CISTAR). The authors thank Hussain Almajed, Dr. Carlos A. Fernandez, Prof. Amaresh Sahu, Prof. Thomas Moore, Prof. Michael Baldea, Dr. Justin Bui, Alex King, and Harrison Lippie for useful discussions.

Author contributions

S.C.D. developed the concept, built the model, and wrote the article. J.R. guided the work. All authors contributed to the discussion, review, and editing of the manuscript.

Competing interests

There are no competing interests to declare.

Data availability

Supplementary information:

Table S1. Capital cost breakdown

Table S2. Operating expense breakdown

Table S3. Base case parameters

Table S4. Ranges in variables for single-variable sensitivity analyses

Table S5. List of universal constants

Table S6. List of symbols used

References

1. Masel, R. I. *et al.* An industrial perspective on catalysts for low-temperature CO2 electrolysis. *Nat. Nanotechnol.* **16**, 118–128 (2021).
2. Guerra, O. J., Almajed, H. M., Smith, W. A., Somoza-Tornos, A. & Hodge, B.-M. S. Barriers and opportunities for the deployment of CO2 electrolysis in net-zero emissions energy systems. *Joule* 1111–1133 (2023) doi:10.1016/j.joule.2023.05.002.
3. Burdyny, T. & Smith, W. A. CO2 reduction on gas-diffusion electrodes and why catalytic performance must be assessed at commercially-relevant conditions. *Energy Environ. Sci.* **12**, 1442–1453 (2019).
4. Torrente-Murciano, L. *et al.* The forefront of chemical engineering research. *Nat. Chem. Eng.* **1**, 18–27 (2024).
5. Smith, W. A., Burdyny, T., Vermaas, D. A. & Geerlings, H. Pathways to Industrial-Scale Fuel Out of Thin Air from CO_2 Electrolysis. *Joule* **3**, 1822–1834 (2019).
6. Da Cunha, S. C. & Resasco, J. Maximizing single-pass conversion does not result in practical readiness for CO2 reduction electrolyzers. *Nat. Commun.* **14**, 5513 (2023).
7. Li, X. *et al.* Greenhouse Gas Emissions, Energy Efficiency, and Cost of Synthetic Fuel Production Using Electrochemical CO_2 Conversion and the Fischer–Tropsch Process. *Energy Fuels* **30**, 5980–5989 (2016).
8. Verma, S., Kim, B., Jhong, H.-R. "Molly", Ma, S. & Kenis, P. J. A. A Gross-Margin Model for Defining Technoeconomic Benchmarks in the Electroreduction of CO_2. *ChemSusChem* **9**, 1972–1979 (2016).
9. Jouny, M., Luc, W. & Jiao, F. General Techno-Economic Analysis of CO_2 Electrolysis Systems. *Ind. Eng. Chem. Res.* **57**, 2165–2177 (2018).

10. Spurgeon, J. M. & Kumar, B. A comparative technoeconomic analysis of pathways for commercial electrochemical CO_2 reduction to liquid products. *Energy Environ. Sci.* **11**, 1536–1551 (2018).
11. De Luna, P. *et al.* What would it take for renewably powered electrosynthesis to displace petrochemical processes? *Science* **364**, eaav3506 (2019).
12. Adnan, M. A. & Kibria, M. G. Comparative techno-economic and life-cycle assessment of power-to-methanol synthesis pathways. *Appl. Energy* **278**, 115614 (2020).
13. Huang, Z., Grim, R. G., Schaidle, J. A. & Tao, L. The economic outlook for converting CO_2 and electrons to molecules. *Energy Environ. Sci.* **14**, 3664–3678 (2021).
14. Shin, H., Hansen, K. U. & Jiao, F. Techno-economic assessment of low-temperature carbon dioxide electrolysis. *Nat. Sustain.* **4**, 911–919 (2021).
15. Do, T. N., You, C. & Kim, J. A CO_2 utilization framework for liquid fuels and chemical production: techno-economic and environmental analysis. *Energy Environ. Sci.* **15**, 169–184 (2022).
16. Sisler, J. *et al.* Ethylene Electrosynthesis: A Comparative Techno-economic Analysis of Alkaline vs Membrane Electrode Assembly vs CO_2–CO–C_2H_4 Tandems. *ACS Energy Lett.* **6**, 997–1002 (2021).
17. Hughes, S. *et al. Sensitivity Analysis Tool for Electrochemical Conversion of CO_2 To CO: User Guide*. DOE/NETL--2024/4405, 2234013 https://www.osti.gov/servlets/purl/2234013/ (2023) doi:10.2172/2234013.
18. Li, W. *et al.* Comparative Techno-Economic and Life Cycle Analysis of Water Oxidation and Hydrogen Oxidation at the Anode in a CO_2 Electrolysis to Ethylene System. *ACS Sustain. Chem. Eng.* **9**, 14678–14689 (2021).

19. Kim, J. *et al.* Design principles for selective and economical CO2 electrolysis in acids. *Appl. Catal. B Environ.* **339**, 123160 (2023).
20. Pribyl-Kranewitter, B., Beard, A., Gîjiu, C. L., Dinculescu, D. & Schmidt, T. J. Influence of low-temperature electrolyser design on economic and environmental potential of CO and HCOOH production: A techno-economic assessment. *Renew. Sustain. Energy Rev.* **154**, 111807 (2022).
21. Raya-Imbernón, A. *et al.* Renewable Syngas Generation via Low-Temperature Electrolysis: Opportunities and Challenges. *ACS Energy Lett.* 288–297 (2023) doi:10.1021/acsenergylett.3c02446.
22. Alerte, T. *et al.* Scale-Dependent Techno-Economic Analysis of CO_2 Capture and Electroreduction to Ethylene. *ACS Sustain. Chem. Eng.* acssuschemeng.3c04373 (2023) doi:10.1021/acssuschemeng.3c04373.
23. Barecka, M. H., Ager, J. W. & Lapkin, A. A. Economically viable CO_2 electroreduction embedded within ethylene oxide manufacturing. *Energy Environ. Sci.* **14**, 1530–1543 (2021).
24. Segets, D., Andronescu, C. & Apfel, U.-P. Accelerating CO2 electrochemical conversion towards industrial implementation. *Nat. Commun.* **14**, 7950 (2023).
25. Debergh, P. *et al.* The Economics of Electrochemical Syngas Production via Direct Air Capture. *ACS Energy Lett.* 3398–3403 (2023) doi:10.1021/acsenergylett.3c00885.
26. Sassenburg, M., Kelly, M., Subramanian, S., Smith, W. A. & Burdyny, T. Zero-Gap Electrochemical CO_2 Reduction Cells: Challenges and Operational Strategies for Prevention of Salt Precipitation. *ACS Energy Lett.* 321–331 (2022) doi:10.1021/acsenergylett.2c01885.

27. Badgett, A. *et al.* An economic analysis of the role of materials, system engineering, and performance in electrochemical carbon dioxide conversion to formate. *J. Clean. Prod.* **351**, 131564 (2022).
28. Hydrogen Analysis Production Models (H2A v3.2018). National Renewable Energy Laboratory.
29. Hawks, S. A. *et al.* Analyzing Production Rate and Carbon Utilization Trade-offs in CO_2RR Electrolyzers. *ACS Energy Lett.* **7**, 2685–2693 (2022).
30. Blake, J. W. *et al.* Inhomogeneities in the Catholyte Channel Limit the Upscaling of CO_2 Flow Electrolysers. *ACS Sustain. Chem. Eng.* **11**, 2840–2852 (2023).
31. Kas, R. *et al.* Along the Channel Gradients Impact on the Spatioactivity of Gas Diffusion Electrodes at High Conversions during CO_2 Electroreduction. *ACS Sustain. Chem. Eng.* **9**, 1286–1296 (2021).
32. Ruthven, D. M., Farooq, S. & Knaebel, K. S. *Pressure Swing Adsorption*. (VCH Publishers, Inc., 1994).
33. Ma, X. *et al.* Carbon monoxide separation: past, present and future. *Chem. Soc. Rev.* **52**, 3741–3777 (2023).
34. Katebah, M., Al-Rawashdeh, M. & Linke, P. Analysis of hydrogen production costs in Steam-Methane Reforming considering integration with electrolysis and CO2 capture. *Clean. Eng. Technol.* **10**, 100552 (2022).
35. Moore, T. *et al.* Electrolyzer energy dominates separation costs in state-of-the-art CO_2 electrolyzers: Implications for single-pass CO_2 utilization. *Joule* **7**, 782–796 (2023).
36. Sinnott, R. & Towler, G. *Chemical Engineering Design*. (Elsevier, 2009). doi:10.1016/C2017-0-01555-0.

37. *Electricity Data Browser*. https://www.eia.gov/electricity/data/browser/ (2023).
38. Boccard, N. Capacity factor of wind power realized values vs. estimates. *Energy Policy* **37**, 2679–2688 (2009).
39. Bolinger, M., Seel, J. & Robson, D. *Utility-Scale Solar: Empirical Trends in Project Technology, Cost, Performance, and PPA Pricing in the United States: 2019 Edition*. https://eta-publications.lbl.gov/sites/default/files/lbnl_utility_scale_solar_2019_edition_final.pdf (2019).
40. Verma, S., Lu, S. & Kenis, P. J. A. Co-electrolysis of CO2 and glycerol as a pathway to carbon chemicals with improved technoeconomics due to low electricity consumption. *Nat. Energy* **4**, 466–474 (2019).
41. Liu, Z., Yang, H., Kutz, R. & Masel, R. I. CO_2 Electrolysis to CO and O_2 at High Selectivity, Stability and Efficiency Using Sustainion Membranes. *J. Electrochem. Soc.* **165**, J3371–J3377 (2018).
42. Weng, L.-C., Bell, A. T. & Weber, A. Z. Towards membrane-electrode assembly systems for CO2 reduction: a modeling study. *Energy Environ. Sci.* **12**, 1950–1968 (2019).
43. Gottesfeld, S. *et al.* Anion exchange membrane fuel cells: Current status and remaining challenges. *J. Power Sources* **375**, 170–184 (2018).
44. Springer, T. E., Zawodzinski, T. A. & Gottesfeld, S. Polymer Electrolyte Fuel Cell Model. *J. Electrochem. Soc.* **138**, 2334–2342 (1991).
45. George, C. Carbon Monoxide. in *Kirk-Othmer Encyclopedia of Chemical Technology* (ed. Kirk-Othmer) (Wiley, 2001). doi:10.1002/0471238961.0301180216090518.a02.pub2.

46. Wesley Cole, A. Will Frazier, & Chad Augustine. *Cost Projections for Utility-Scale Battery Storage: 2021 Update*. https://www.nrel.gov/docs/fy21osti/79236.pdf (2021).

47. Bilicic, G. & Scroggins, S. *Lazard's Levelized Cost of Energy Analysis — Version 16.0*. https://www.lazard.com/research-insights/2023-levelized-cost-of-energyplus/ (2023).

48. Lees, E. W., Bui, J. C., Romiluyi, O., Bell, A. T. & Weber, A. Z. Exploring CO2 reduction and crossover in membrane electrode assemblies. *Nat. Chem. Eng.* **1**, 340–353 (2024).

49. Bagemihl, I., Cammann, L., Pérez-Fortes, M., Van Steijn, V. & Van Ommen, J. R. Techno-economic Assessment of CO_2 Electrolysis: How Interdependencies between Model Variables Propagate Across Different Modeling Scales. *ACS Sustain. Chem. Eng.* **11**, 10130–10141 (2023).

50. Corral, D. *et al.* Advanced manufacturing for electrosynthesis of fuels and chemicals from CO_2. *Energy Environ. Sci.* **14**, 3064–3074 (2021).

51. Gabardo, C. M. *et al.* Continuous Carbon Dioxide Electroreduction to Concentrated Multi-carbon Products Using a Membrane Electrode Assembly. *Joule* **3**, 2777–2791 (2019).

52. Wheeler, D. G. *et al.* Quantification of water transport in a CO_2 electrolyzer. *Energy Environ. Sci.* **13**, 5126–5134 (2020).

53. O'Brien, C. P. *et al.* Single Pass CO_2 Conversion Exceeding 85% in the Electrosynthesis of Multicarbon Products via Local CO_2 Regeneration. *ACS Energy Lett.* **6**, 2952–2959 (2021).

54. Garg, S. *et al.* Advances and challenges in electrochemical CO2 reduction processes: an engineering and design perspective looking beyond new catalyst materials. *J. Mater. Chem. A* **8**, 1511–1544 (2020).

55. Subramanian, S. *et al.* Geometric Catalyst Utilization in Zero-Gap CO_2 Electrolyzers. *ACS Energy Lett.* 222–229 (2022) doi:10.1021/acsenergylett.2c02194.

56. Wan, S. *et al.* Improving the Efficiencies of Water Splitting and CO $_2$ Electrolysis by Anodic O $_2$ Bubble Management. *J. Phys. Chem. Lett.* **14**, 11217–11223 (2023).

57. Lin, R., Lu, Y., Xu, J., Huo, J. & Cai, X. Investigation on performance of proton exchange membrane electrolyzer with different flow field structures. *Appl. Energy* **326**, 120011 (2022).

58. Hori, Y. Electrochemical CO2 Reduction on Metal Electrodes. in *Modern Aspects of Electrochemistry* (eds. Vayenas, C. G., White, R. E. & Gamboa-Aldeco, M. E.) vol. 42 89–189 (Springer New York, New York, NY, 2008).

59. Murata, A. & Hori, Y. Product Selectivity Affected by Cationic Species in Electrochemical Reduction of CO2 and CO at a Cu Electrode. *Bull. Chem. Soc. Jpn.* **64**, 123–127 (1991).

60. Edwards, J. P. *et al.* Pilot-Scale CO_2 Electrolysis Enables a Semi-empirical Electrolyzer Model. *ACS Energy Lett.* 2576–2584 (2023) doi:10.1021/acsenergylett.3c00620.

61. Seider, W. D. *et al. Product and Process Design Principles: Synthesis, Analysis and Evaluation*. (Wiley, New York, 2017).

62. David Peterson, James Vickers, & Dan DeSantis. *Hydrogen Production Cost from PEM Electrolysis - 2019*. https://www.hydrogen.energy.gov/docs/hydrogenprogramlibraries/pdfs/19009_h2_production_cost_pem_electrolysis_2019.pdf?Status=Master (2020).